Contents lists available at ScienceDirect

Ultrasonics Sonochemistry

journal homepage: www.elsevier.com/locate/ultson

Decolorization of azo dye Orange G by aluminum powder enhanced by ultrasonic irradiation

Mei Qiang Cai [a],*, Xiao Qin Wei [a], Zhi Jun Song [a], Mi Cong Jin [b,c],*

[a] School of Environmental Science and Engineering, Zhejiang Gongshang University, Hangzhou 310018, China
[b] Zhejiang Provincial Key Laboratory of Health Risk Appraisal for Trace Toxic Chemicals, Ningbo Municipal Center for Disease Control and Prevention, Ningbo 315010, China
[c] Ningbo Key Laboratory of Poison Research and Control, Ningbo Municipal Center for Disease Control and Prevention, Ningbo 315010, China

ABSTRACT

In this work, the decolorization of azo dye Orange G (OG) in aqueous solution by aluminum powder enhanced by ultrasonic irradiation (AlP-UI) was investigated. The effects of various operating operational parameters such as the initial pH, initial OG concentration, AlP dosage, ultrasound power and added hydrogen peroxide (H_2O_2) concentration were studied. The results showed that the decolorization rate was enhanced when the aqueous OG was irradiated simultaneously by ultrasound in the AlP-acid systems. The decolorization rate decreased with the increase of both initial pH values of 2.0–4.0 and OG initial concentrations of 10–80 mg/L, increased with the ultrasound power enhancing from 500 to 900 W. An optimum value was reached at 2.0 g/L of the AlP dosage in the range of 0.5–2.5 g/L. The decolorization rate enhanced significantly by the addition of hydrogen peroxide in the range of 10–100 mM to AlP-UI system reached an optimum value of 0.1491 min^{-1}. The decolorization of OG appears to involve primarily oxidative steps, the cleavage of N=N bond, which were verificated by the intermediate products of OG under the optimal tested degradation system, aniline and 1-amino-2-naphthol-6,8-disulfonate detected by the LC–MS.

© 2014 Elsevier B.V. All rights reserved.

1. Introduction

Azo dye is a significant part of synthetic textile dyes and represents the largest class of dyes applied in textile processing. The azo dyes are poorly biodegradable pollutants with toxicity, mutagenicity and carcinogenicity, and have aroused a serious environmental problem because of these characteristics. The traditional treatment techniques include physical, chemical, and biological treatment, such as adsorption [1–3], coagulation [4], photo-catalysis [5,6], ozonation [7], and biosorption [8–10], however, these treatments are usually high costs, time-consuming, and limited applicability.

Advanced oxidation processes (AOPs) can be defined broadly as the processes that generate and attack of the hydroxyl radicals in sufficient quantities to oxidize a wide range of organic chemicals in wastewater. Hydroxyl radicals are powerful oxidizing reagents with an oxidation potential of 2.33 V, which is substantially higher than other oxidants such as hydrogen peroxide, permanganate

ions, etc. AOPs involving the Fenton reaction [11,12], wet air oxidation [13], ozonation [14,15], electrolysis [16], photolysis [17,18], cavitation [19,20], radiolysis [21], ultrasonic irradiation [22–24], ultraviolet (UV) radiation [25] and their combinations [26–29] are widely studied for the decomposition of large kinds of hazardous organic compounds.

Ultrasonic irradiation is considered as an advanced oxidation process since hydroxyl radicals are generated as a result of ultrasonic cavitation. The ultrasonic cavitation is created by the ultrasonic waves in the range of 20–1000 kHz being transmitted throughout an aqueous solution in a sonochemical process or sonolysis [30]. The ultrasonic cavitation is defined as the formation, growth, and subsequent implosive collapse of vapor or gas filled cavities occurring in an extremely small interval of time, releasing enormous magnitudes of energy [31,32]. During the collapse process, the hydrophobic volatile organic pollutants in water can undergo high-temperature pyrolysis in the gas phase inside the bubbles, and the non-volatile, hydrophilic species can be degraded by ·OH at the bubble surface or in bulk solution. Besides chemical effects, ultrasound irradiation can also produce a number of physical effects such as microstreaming, microjets, shock waves [32,33]. However, the use of ultrasonic cavitation reactors at large scale poses critical problems such as lower energy efficiencies and

* Corresponding authors. Tel.: +86 571 88071024x7056; fax: +86 571 28008215 (M.Q. Cai). Address: Zhejiang Provincial Key Laboratory of Health Risk Appraisal for Trace Toxic Chemicals, Ningbo Municipal Center for Disease Control and Prevention, Ningbo 315010, China. Tel.: +86 574 87274559; fax: +86 574 87361764 (M.C. Jin).
E-mail addresses: caimeiqiang@163.com (M.Q. Cai), jmcjc@163.com (M.C. Jin).

higher investment costs [34,35]. Moreover, the process of ultrasonic cavitation usually takes a long processing time in order to achieve complete mineralization of pollutants.

The combination of ultrasound irradiation and other different AOPs such as photocatalytic oxidation [36], electrochemical [37], ozonation [38,39], and particularly advanced Fenton process and Fenton like processes [40] has been reported to be much more efficient and promising for the oxidative removal of organic pollutants than the treatment alone. In the recent past, less attention has been paid to the reductive degradation using the zero-valent aluminum (ZVAl). The ZVAl is a strong reducing agent (E^0 = −1.662 V) that has a standard reduction potential more negative than zero-valent iron (E^0 = −0.43 V) [41,42]. As well as the zero-valent iron, the degradation capable of ZVAl also rely on the amounts of in situ generation of reactive oxygen species (ROS) including hydrogen peroxide (H_2O_2), superoxide radical ($O_2^{\cdot-}$), and hydroxyl radical ($\cdot OH$), which are capable of oxidizing contaminants that cannot be well removed by ZVAl reductively. The mechanism of the ZVAl to form hydroxyl radical could be described as follows [43,44]:

$$2Al^0 + 3O_2 + 6H^+ \rightarrow 2Al^{3+} + 3H_2O_2 \tag{1}$$

$$Al^0 + 3H_2O_2 \rightarrow Al^{3+} + 3\cdot OH + 3OH^- \tag{2}$$
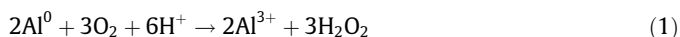
First, it can be seen that the reduction of O_2 on zero valent aluminum (Al^0) in the acid conditions leads to form H_2O_2 and subsequently generate $\cdot OH$ via Fenton like reactions (Eqs. (1) and (2)). Surprisingly, to the best of our knowledge, no reports on the pollutant degradation using the combination of ZVAl and ultrasonic irradiation (ZVAl–UI) can be found. As expected, the formed H_2O_2 both in the interface of gaseous bubble and in solution (Eqs. (3) and (4)) due to the pyrolysis of water can be utilized to produce more amounts of hydroxyl radicals by reaction with ZVAl. Consequently, the ZVAl–UI process should be a suitable method to increase the efficiency of degradation process:

$$H_2O+))) \rightarrow \cdot OH + \cdot H \tag{3}$$

$$\cdot OH + \cdot OH \rightarrow H_2O_2 \tag{4}$$

Orange G (OG) is a typical reactive azo dye and extensively used in the dyeing of textile fabrics. The chemical structure of OG is shown in Fig. 1. The decolorization methods of OG in wastewater including adsorption [45,46], sonolysis [47], biotransformation [48], UV/TiO₂ [49,50] and Fenton processes [51] had been reported. However, there are no reports about the decolorization of OG via the ZVAl under ultrasonic irradiation. In general, the surface of Al is covered with oxide film due to oxidizability of ZVAl, and the hydrochloric acid solution is usually used to remove the oxide film,
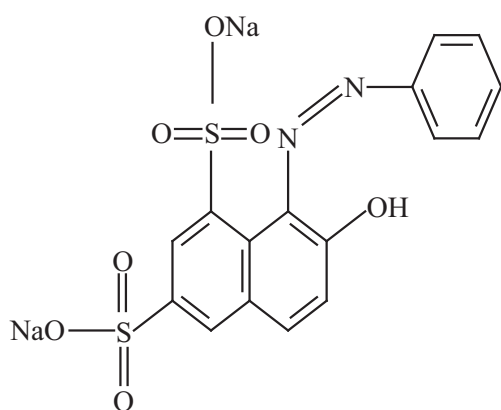
Fig. 1. Molecular structure of azo dye Orange G.

which is not suitable in practice [39]. As mentioned above, ultrasonic irradiation provides a straightforward method of using AlP instead of ZVAl due to the chemical and physical effects of ultrasound irradiation. This prompted us first to study decolorization of azo dye Orange G using AlP-UI. The results are expected to provide fundamental knowledge for the treatment of wastewater containing hydrophilic pollutants via AlP-UI. The effects of various operating operational parameters including the initial pH, initial OG concentration, AlP dosage, ultrasound power and added H_2O_2 concentration were studied.

2. Experimental

2.1. Chemicals and solvents

Orange G and hydrogen peroxide were purchased from Huipu Chemical&Apparatus Co. (Hangzhou, China). Aluminum powder (purity >99%, particle size 38–48 μm, surface covered with native aluminum oxide layer) were obtained from Kelon Chem. (Shanghai, China). Other reagents with analytical grade or high performance liquid chromatography (HPLC) grade were obtained from Huipu Chemical&Apparatus Co. (Hangzhou, China). The concentration of the purchased hydrogen peroxide (H_2O_2) solution (30 wt.%) was calibrated by titration with potassium permanganate [52]. All chemicals were used as received. The water employed was supplied by a Milli-Q water purification system from Millipore (Molsheim, France).

2.2. Experimental methodology

The decolorization of OG using the UI, AlP-acid and AlP-UI were carried out under different conditions. An ultrasonic immersion-probe liquid processor (TJS-3000, Fuyang Chenggong Ultrasonic Co., China) with tapered type titanium probe (1.6 cm diameter) operating at 20 kHz was used for the decolorization experiments by the UI and AlP-UI. The ultrasonic electrical power was in the range of 0–900 W. All reactions with a total suspension volume of 250 mL for 180 min were carried out in 500 mL double walled-type reactor and water was circulated between the walls in order to keep the temperature constant at 25 ± 1 °C. Samples were collected at designated time intervals and filtered using membrane filters (0.45 μm pore size). The concentration of OG was analyzed by measuring the absorbance of dye solution at 478 nm using a TU-1901 UV-spectrophotometer (Persee General Co., Beijing, China). All experiments were repeated three times and the average values are reported. The temperature of reaction systems was continuously monitored at about 25 ± 1 °C by a thermocouple connected to a digital thermometer (DS18B20, Dallas Crop, USA).

Hydrogen production experiments of the reaction of aluminum powder, sodium hydroxide and water were conducted to check the peel effect of ultrasonic irradiation. The method and equipment used to quantify hydrogen production yields were similar to the reference [53]. In these experiments, the used aluminum powder were washed thrice for 5 min in 0.1 mol/L of hydrochloric acid (HCl) in order to remove the surface oxidation layers, rinsed with deionized water, and dried at 30 °C under an Ar atmosphere.

2.3. Detection technique

The OG decolorization products were determined by an Agilent 1100 series LC/MSD Trap SL System (Agilent Technologies Inc., Germany), consisting of a quaternary pump (G1311A), a column thermostat (G1316A), a degasser unit (G1379A), an autosampler (G1313A), and an ion trap mass spectrometer with an electrospray ion (ESI) source. The LC/MSD Trap SL system was controlled, and

data were analyzed, with a computer equipped with LC/MSD Trap Software 4.2 (Bruker). The chromatographic separation was carried out on a Phenomenx Gemini C18 column (150 mm × 2.0 mm i.d., 5 μm) by using a mixture of acetonitrile/10 mmol/L ammonium acetate solution (20:70, v/v) as the mobile phase in isocratic eluent at a constant flow rate of 0.25 mL/min. The column temperature was held at 30 °C, and the injection volume was 25 μL. MS detection was performed in positive ESI mode with a full scan mass spectrum over the m/z range 50–500. The operating conditions for ESI were dry gas (nitrogen) pressure 60 psi, auxiliary gas (nitrogen) flow 9.0 L/min, a capillary voltage 3.5 kV, capillary temperature 325 °C and dwell time 200 ms.

3. Results and discussion

3.1. Decolorization by three different treatments

The decolorization of OG was investigated using three different treatments including UI, AlP-acid and AlP-UI. The experiments were investigated when the initial OG concentration is 10 mg/L, initial pH value is 3.0, AlP dosage is 2.0 g/L and ultrasound power is 900 W. As shown in Fig. 2, the decolorization efficiency of OG by AlP-UI within 180 min was 62.4%, which was higher that of 22.0% and 37.3%, for AlP-acid and UI, respectively. The decolorization rate of 0.0057 min^{-1} under AlP-UI was also much higher 0.0042 min^{-1} of the sum of 0.0028 min^{-1} and 0.0014 min^{-1} by UI and AlP-acid, respectively, showing a certain synergistic effect. The observed synergistic effect is attributed to the increasing amount of hydroxyl radicals. Under the single UI, the formed H_2O_2 both in the interface of gaseous bubble and solution are unavailability for hydrophilic azo dye OG. However, in the AlP-UI system, these hydrogen peroxides are utilized to produce hydroxyl radicals by the reaction with the ZVAl which are oxidized to Al^{3+} as shown in Eq. (2). Moreover, the covered aluminum oxide can also used to generate hydroxyl radicals by providing contact sites for these hydrogen peroxides, which is widely used in the hydrogen peroxide production via anthraquinone [54]. Furthermore, the UI increase the decomposition of the AlP-induced H_2O_2. Liu et al. [55] found that although up to 51 mmol/L H_2O_2 was generated in the AlP-acid system, no bisphenol A was removed over the 12 h reaction, indicating that the transformation of the formed H_2O_2 to OH radical is not immediately happened. However, when hydrogen peroxide was subjected to UI, the cavitation-induced thermal effect accelerate the decomposition of hydrogen peroxide to reactive species [56]. However, the decolorization rate was lower than

0.01347 min^{-1} obtained at our lab under Sono-Fenton like reaction at the OG initial concentration of 10 mg/L, initial pH value of 3, Fe_0 concentration of 500 mg/L, ultrasonic power of 300 W. This may due to the covered oxide film at the surface of Al.

3.2. Effect of initial pH value

The effect of different initial pH value of solution on the decolorization rate of OG was investigated at different pH in the range 2.0–4.0 with initial OG concentration of 10 mg/L, AlP concentration of 2.0 g/L, ultrasound of 900 W. As shown in Fig. 3, the rate of decolorization increases with the decreasing initial solution pH, indicating that acidic conditions is much more suitable for the decolorization of OG dye. The decolorization efficiency of 98.8% within 120 min was achieved at pH value of 2.0. There was very little difference in removal value between pH at 2.0 and 2.5 within 180 min, the decolorization efficiency within 180 min was 71.2%, 67.0% and 51.1% at pH 3.0, 3.5, 4.0, respectively, which are considerably lower than that obtained at pH 2.0. The decolorization rate of 0.0499 min^{-1} at pH 2.0 is much higher than 0.0249 min^{-1} at pH 2.5 in 120 min. These observed experimental results can be explained as follows: first, the formation and accumulation of OH radicals in the liquid bulk produced from H_2O_2 dissociation under sonolysis is much higher at pH = 2 than pH = 4.0, which contributes to the comparably higher decolorization rate [57]. It was widely reported that the lower pH is more favorable to degrade organic dyes [58,59]. Secondly, the production of OH radicals induced from ZVAl (Eqs. (1) and (2)) is also highly favored under acidic conditions. Similar results that the degradation is more effective under pH < 3.5 acidic conditions in ZVAl–UI system were also reported [39]. Hydrogen production experiments of the reaction of aluminum powder, sodium hydroxide and water were conducted using 5 g aluminum powder treated using 0.1 M HCl solution as mentioned in the experimental section and treated using 10 min of 900 W UI at pH of 2.0, and non-treated AlP, respectively. The results showed that about more 1.67 and 1.12 L hydrogen gas was produced using acid-treated AlP and UI-treated AlP, respectively, than that of non-treated AlP which produce about 4.69 L hydrogen gas under atmospheric pressure. This result indicated that the non-treated aluminum powders are consist of zero valent Al and aluminum powders covered with oxide film. Using the UI-treated AlP at pH of 2.0 as the aluminum resource, more 0.89 L hydrogen gas was produced than that of at pH of 4.0. This result also indicated that the lower pH is more favorable to peel the
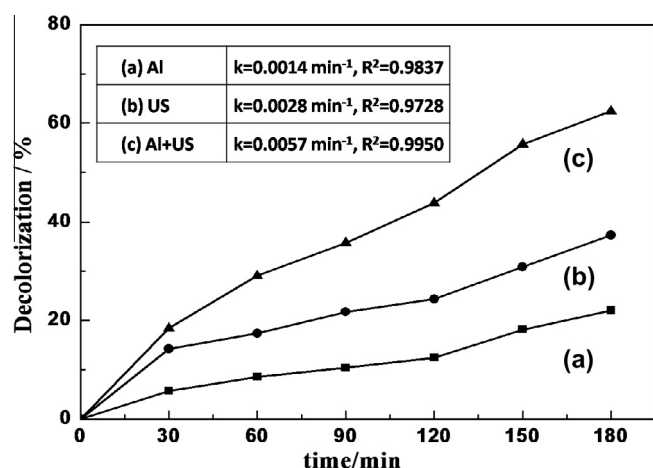
Fig. 2. Decolorization of Orange G using three different processes. (Experimental conditions: [AlP] = 2.0 g/L, [OG]$_0$ = 10 mg/L; pH = 3.0, ultrasound power = 900 W.)
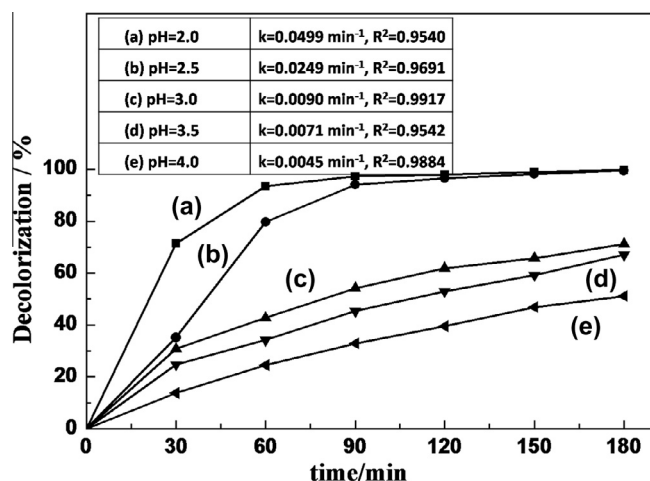
Fig. 3. Effect of initial pH on the decolorization rate of Orange G. (Experimental conditions: [AlP] = 2.0 g/L, [OG]$_0$ = 10 mg/L, ultrasound power = 900 W.)

aluminum powder covered with oxide film to zero valent Al for ultrasonic irradiation.

3.3. Effect of initial Orange G concentration

The effect of OG initial concentrations in the range of 10.0–80.0 mg/L on the decolorization rate was also investigated at pH 3.0, ZVAl concentration 2.0 g/L, ultrasonic power 900 W. As shown in Fig. 4, the decolorization efficiency decrease with the increasing initial OG concentration within 180 min. The decolorization efficiency decrease from 71.2% to 34.2%, and decolorization rate decrease from 0.090 to 0.025 min^{-1} as the initial concentration of OG increase from 10 to 80 mg/L. The main mechanisms of the decolorization of OG is the reactions of hydroxyl radicals with the N≡N bond with generation of nitrosoaryl intermediates or the C—N bond resulting in aniline as one of the intermediate products in bulk solution [60,61]. Generally, the concentration of non-surfactant hydrophilic OG will not change the amounts of generated-OH radicals concentration [62]. The increasing OG concentration will change the ratio of OG to OH radicals. When the ratio reaches a certain values, the further increasing OG concentrations will cause no significant change in decolorization rate.

3.4. Effect of zero valent aluminum dosage

In order to study the effect of AlP dosage, five different AlP dosages in the range from 0.5 to 2.5 g/L in 250 mL aqueous solution were investigated when the initial pH value is 3.0, OG concentration is 10 mg/L, ultrasonic power is 900 W. As shown in Fig. 5, the decolorization efficiency increase from 62.4% to 71.2%, and the decolorization rate increase from 0.0057 min^{-1} to 0.0090 min^{-1} with the increasing of AlP dosage from 0.5 g/L to 2.0 g/L. The AlP dosage of 2.0 g/L was found to be optimum in the OG decolorization. The decolorization efficiency and decolorization rate decrease beyond the AlP dosage of 2.0 g/L. The enhanced OG decolorization rates with higher AlP loadings is due to the increase of reaction surface area of AlP, which support more reactive sites to produce the ·OH radicals for cavitation-induced and AlP-induced H_2O_2. However, the decolorization rate decrease when the AlP loading was >2.0 g/L, which may due to the facts including both dissolution of native oxide layer and corrosion of AlP and metal aluminum led to Al^{3+}, H_2, $Al(OH)_3$ and H^+ (Eqs. (5) and (6)), which affect the cavitation events and the cavitation-induced ·OH and H_2O_2:
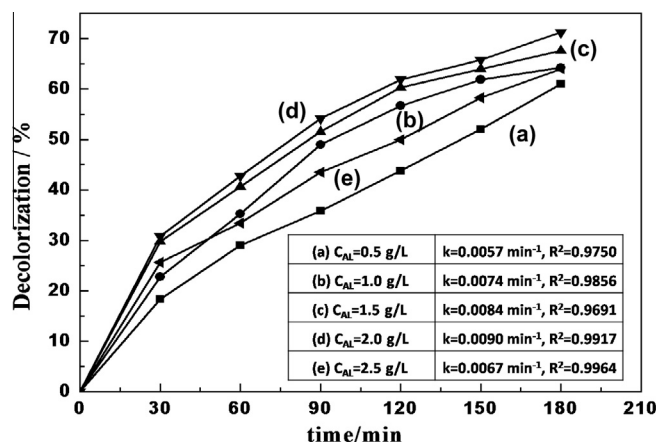
Fig. 5. Effect of aluminum powder dosage on the decolorization rate of Orange G. (Experimental conditions: $[OG]_0$ = 10 mg/L, pH = 3.0, ultrasound power = 900 W.)

(a) C_{Al}=0.5 g/L	k=0.0057 min^{-1}, R^2=0.9750	
(b) C_{Al}=1.0 g/L	k=0.0074 min^{-1}, R^2=0.9856	
(c) C_{Al}=1.5 g/L	k=0.0084 min^{-1}, R^2=0.9691	
(d) C_{Al}=2.0 g/L	k=0.0090 min^{-1}, R^2=0.9917	
(e) C_{Al}=2.5 g/L	k=0.0067 min^{-1}, R^2=0.9964	
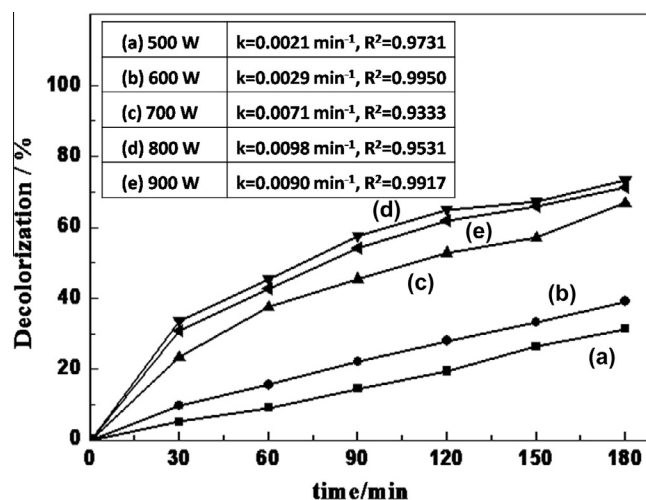
Fig. 6. Effect of ultrasound power on the decolorization rate of Orange G. (Experimental conditions: $[OG]_0$ = 10 mg/L, pH = 3.0, [AlP] = 2.0 g/L.)

(a) 500 W	k=0.0021 min^{-1}, R^2=0.9731
(b) 600 W	k=0.0029 min^{-1}, R^2=0.9950
(c) 700 W	k=0.0071 min^{-1}, R^2=0.9333
(d) 800 W	k=0.0098 min^{-1}, R^2=0.9531
(e) 900 W	k=0.0090 min^{-1}, R^2=0.9917
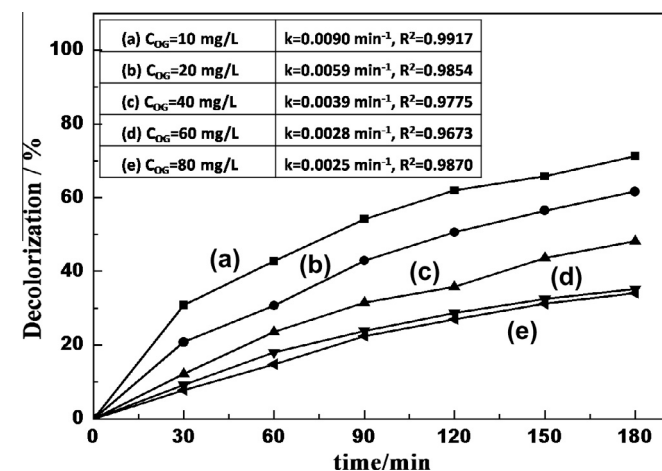
Fig. 4. Effect of Orange G initial concentration on the decolorization rate. (Experimental conditions: [AlP] = 2.0 g/L, pH = 3.0, ultrasound power = 900 W.)

(a) C_{OG}=10 mg/L	k=0.0090 min^{-1}, R^2=0.9917
(b) C_{OG}=20 mg/L	k=0.0059 min^{-1}, R^2=0.9854
(c) C_{OG}=40 mg/L	k=0.0039 min^{-1}, R^2=0.9775
(d) C_{OG}=60 mg/L	k=0.0028 min^{-1}, R^2=0.9673
(e) C_{OG}=80 mg/L	k=0.0025 min^{-1}, R^2=0.9870
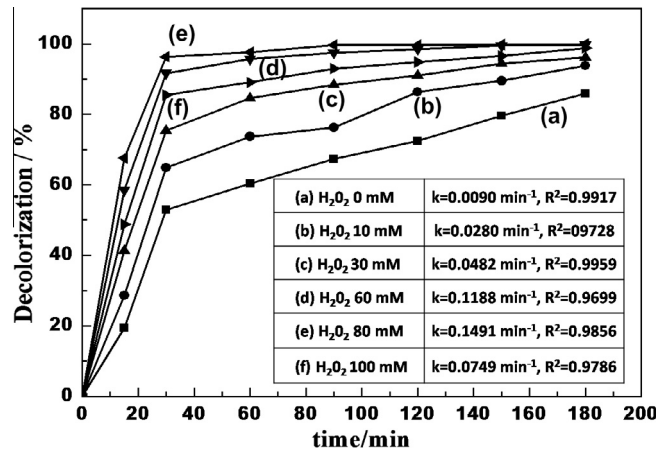
Fig. 7. Effect of H_2O_2 concentration on the decolorization rate of Orange G. (Experimental conditions: $[OG]_0$ = 10 mg/L, pH = 3.0, [AlP] = 2.0 g/L, ultrasound power = 900 W.)

(a) H_2O_2 0 mM	k=0.0090 min^{-1}, R^2=0.9917
(b) H_2O_2 10 mM	k=0.0280 min^{-1}, R^2=09728
(c) H_2O_2 30 mM	k=0.0482 min^{-1}, R^2=0.9959
(d) H_2O_2 60 mM	k=0.1188 min^{-1}, R^2=0.9699
(e) H_2O_2 80 mM	k=0.1491 min^{-1}, R^2=0.9856
(f) H_2O_2 100 mM	k=0.0749 min^{-1}, R^2=0.9786
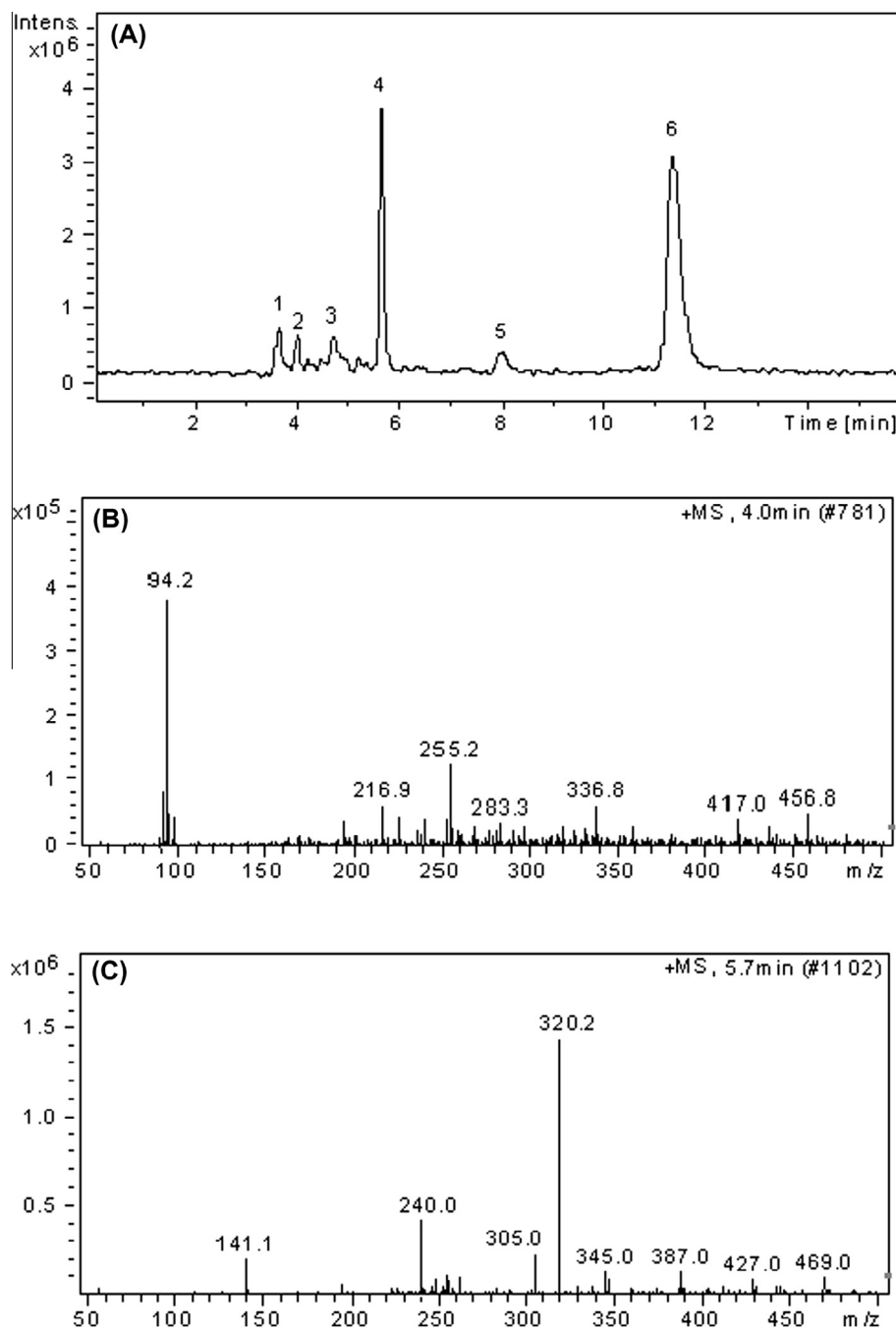
Fig. 8. The total ion chromatogram (TIC) of the OG decolorization solution by LC–MS in the positive ESI mode (A), the mass spectrometry of the peak at the run time of 4.0 min (B), and the mass spectrometry of the peak at the run time of 5.7 min (C). In (A), peak 1: unknown, 2: aniline, 3: unknown, 4: 1-amino-2-naphthol-6,8-disulfonate, 5: unknown, 6: OG.

$$2Al + 6H^+ \rightarrow 2Al^{3+} + 3H_2 \uparrow \qquad (5)$$

$$Al^{3+} + 3H_2O \rightarrow Al(OH)_3 + 3H^+ \qquad (6)$$

3.5. Effect of ultrasound power

The effect of ultrasound power in the range from 500 to 900 W on the decolorization rate was investigated at pH = 3.0, the initial OG concentration is 10 mg/L, the AlP concentration is 2.0 g/L, and the results were shown in Fig. 6. As can be seen from Fig. 6, both the decolorization efficiency and rate increase up to optimum

and then remained almost unchanged. This result is similar to other reported studies [39,63,64]. As mentioned above, the decolorization of OG is ·OH dependent. The increasing acoustic power increase the number of active cavitation bubbles, and result in the higher collapse temperature and more OH radicals [65–67]. In addition, the cavitation-induced effects including acoustic microstreaming increase the surface area and reactivity of AlP, and improve the mass transport of the reactants and by-products by cleaning and sweeping of the AlP surface [68]. In the other hand, at higher acoustic power with larger values in acoustic amplitude, the cavitation bubbles grow during the rarefaction cycle to the very large values of the maximum radius, but are unable to undergo

complete collapse during the compression phase due to insufficient collapse times. Therefore, these bubbles are not transient, and continue to either oscillate under stable cavitation conditions, or grow large enough to escape from the liquid through buoyancy and mass convection [66]. Briefly, the increase of UI power also leads to the insufficient collapse of the cavitation bubbles and reduce the amount of OH radicals.

3.6. Effect of the H_2O_2 addition

The addition of hydrogen peroxide used as an effective source of hydroxyl radicals is an important parameter for the enhancement of decolorization rate. In this work, five H_2O_2 addition concentrations between 0 and 100 mmol/L on the decolorization rate were investigated when the initial pH = 3, AlP concentration is 2.0 g/L, ultrasound power is 900 W. As shown in Fig. 7, the decolorization efficiency and rate increase with the increasing H_2O_2 addition from 0 to 80 mmol/L and decrease beyond the H_2O_2 addition of 80 mmol/L. The result indicates that there is an optimum concentration of H_2O_2 for the decolorization of OG dye. The addition of hydrogen peroxide can be attributed to an effective source of OH radicals and a higher cavitational intensity, which leads to the formation of a higher amount of OH radicals [69]. However, the excessive H_2O_2 as radical scavenger also can reduce the amounts of effective OH radicals [70].

3.7. Detection of the decolorization products

Fig. 8 shows the total ion chromatogram (TIC) of the OG decolorization solution, which was decolorized under the optimal tested degradation system for 30 min, by LC–MS in the positive ESI mode. It can be seen that aniline and 1-amino-2-naphthol-6,8-disulfonate are detected at the run time of 4.0 min and 5.7 min, respectively. Both compounds were derived from the breakage of the N=N bond in OG molecule, and also verificated that the decolorization of OG appears to involve the primarily oxidative cleavage of N=N bond.

4. Conclusion

The aluminum powder-acid system irradiated by ultrasound is an effective method for the decolorization of azo dye OG in aqueous solution. The decolorization rate is dependent on the operating parameters including the initial pH, initial OG concentration, AlP dosage and ultrasound power. The decolorization rate can be enhanced significantly by the addition of hydrogen peroxide due to the additional hydroxyl radicals. More work is required to determine the precise mechanism based on detection results of decolorization products, which can provide fundamental knowledge for the treatment of wastewater containing OG and/or other azo dyes by the AlP-UI process.

Acknowledgments

References

[1] V.K. Gupta, B. Gupta, A. Rastogi, S. Agarwal, A. Nayak, A comparative investigation on adsorption performances of mesoporous activated carbon prepared from waste rubber tire and activated carbon for a hazardous azo dye-Acid Blue, J. Hazard. Mater. 186 (2011) 891–901.

[2] S. Papic, N. Koprivanac, A. Loncaric Bozic, A. Metes, Removal of some reactive dyes from synthetic wastewater by combined Al (III) coagulation/carbon adsorption process, Dyes Pigments 62 (2004) 291–298.

[3] C.L. Yang, J. McGarrahan, Electrochemical coagulation for textile effluent decolorization, J. Hazard. Mater. 127 (2005) 40–47.

[4] E. Ellouze, D. Ellouze, A. Jrad, R. Ben Amar, Treatment of synthetic textile wastewater by combined chemical coagulation/membrane processes, Desalination 33 (2011) 118–124.

[5] T.A. Saleh, V.K. Gupta, Photo-catalyzed degradation of hazardous dye methyl orange by use of a composite catalyst consisting of multi-walled carbon nanotubes and titanium dioxide, J. Colloid Interface Sci. 371 (2012) 101–106.

[6] A.R. Khataee, M.N. Pons, O. Zahraa, Photocatalytic degradation of three azo dyes using immobilized TiO$_2$ nanoparticles on glass plates activated by UV light irradiation: influence of dye molecular structure, J. Hazard. Mater. 168 (2009) 451–457.

[7] C.P. Bai, X.F. Xiong, W.Q. Gong, D.X. Feng, M. Xian, Z.X. Ge, N. Xu, Removal of rhodamine B by ozone-based advanced oxidation process, Desalination 278 (2011) 84–90.

[8] A.H. Chen, S.M. Chen, Biosorption of azo dyes from aqueous solution by glutaraldehyde-crosslinked chitosans, J. Hazard. Mater. 172 (2009) 1111–1121.

[9] F. Elisangela, Z. Andrea, D.G. Fabio, R.D.M. Cristiano, D.L. Regina, C.P. Artur, Biodegradation of textile azo dyes by a facultative *Staphylococcus arlettae* strain VN-11 using a sequential microaerophilic/aerobic process, Int. Biodeter. Biodegrad. 63 (2008) 280–288.

[10] O. Türgay, G. Ersöz, S. Atalay, J. Forss, U. Welander, The treatment of azo dyes found in textile industry wastewater by anaerobic biological method and chemical oxidation, Sep. Purif. Technol. 79 (2011) 26–33.

[11] A. Özcan, M.A. Oturan, N. Oturan, Y. Sahin, Removal of acid Orange 7 from water by electrochemically generated Fenton's reagent, J. Hazard. Mater. 163 (2009) 1213–1220.

[12] A. Rastogi, S.R. Al-Abed, D.D. Dionysiou, Effect of inorganic, synthetic and naturally occurring chelating agents on Fe (II) mediated advanced oxidation of chlorophenols, Water Res. 43 (2009) 684–694.

[13] H.T. Gomes, S.M. Miranda, M.J. Sampaio, A.M.T. Silva, J.L. Faria, Activated carbons treated with sulphuric acid: catalysts for catalytic wet peroxide oxidation, Catal. Today 151 (2010) 153–158.

[14] M. Koch, A. Yediler, D. Lienert, G. Insel, A. Kettrup, Ozonation of hydrolyzed azo dye reactive yellow 84 (CI), Chemosphere 46 (2002) 109–113.

[15] H.Y. Li, J.H. Qu, H.J. Liu, Decomposition of alachlor by ozonation and its mechanism, J. Environ. Sci. 19 (2007) 769–775.

[16] N. Daneshvar, D. Salari, A.R. Khataee, Photocatalytic degradation of azo dye acid red 14 in water: investigation of the effect of operational parameters, J. Photochem. Photobiol. A 157 (2003) 111–116.

[17] M. Mrowetz, C. Pirola, E. Selli, Degradation of organic water pollutants through sonophotocatalysis in the presence of TiO$_2$, Ultrason. Sonochem. 10 (2003) 247–254.

[18] C.K. Duesterberg, W.J. Cooper, T.D. Waite, Fenton-mediated oxidation in the presence and absence of oxygen, Environ. Sci. Technol. 39 (2005) 5052–5058.

[19] A.A. Pradhan, P.R. Gogate, Removal of p-nitrophenol using hydrodynamic cavitation and Fenton chemistry at pilot scale operation, Chem. Eng. J. 156 (2009) 77–82.

[20] J.H. Sun, S.P. Sun, J.Y. Sun, R.X. Sun, L.P. Qiao, H.Q. Guo, M.H. Fan, Degradation of azo dye Acid black 1 using low concentration iron of Fenton process facilitated by ultrasonic irradiation, Ultrason. Sonochem. 14 (2007) 761–766.

[21] S.J. Zhang, H.Q. Yu, Q.R. Li, Radiolytic degradation of Acid Orange 7: a mechanistic study, Chemosphere 61 (2005) 1003–1011.

[22] J.J. Pignatello, E. Oliveros, A. MacKay, Advanced oxidation processes for organic contaminant destruction based on the Fenton reaction and related chemistry, Crit. Rev. Environ. Sci. Technol. 36 (2006) 1–84.

[23] M. Chiha, S. Merouani, O. Hamdaoui, S. Baup, N. Gondrexon, C. Pétrier, Modeling of ultrasonic degradation of non-volatile organic compounds by Langmuir-type kinetics, Ultrason. Sonochem. 17 (2010) 773–782.

[24] R. Singla, F. Grieser, M. Ashokkumar, Sonochemical degradation of martius yellow dye in aqueous solution, Ultrason. Sonochem. 16 (2009) 28–34.

[25] M.W. Chang, C.C. Chung, J.M. Chern, T.S. Chen, Dye decomposition kinetics by UV/H$_2$O$_2$: initial rate analysis by effective kinetic modeling methodology, Chem. Eng. Sci. 65 (2009) 135–140.

[26] N. Shimizu, C. Ogino, M.F. Dadjour, T. Murata, Sonocatalytic degradation of methylene blue with TiO$_2$ pellets in water, Ultrason. Sonochem. 14 (2007) 184–190.

[27] P.R. Gogate, Treatment of wastewater streams containing phenolic compounds using hybrid techniques based on cavitation: a review of the current status and the way forward, Ultrason. Sonochem. 15 (2007) 1–15.

[28] D.H. Bremner, S.D. Carlo, A.G. Chakinala, G. Cravotto, Mineralization of 2,4-dichlorophenoxyacetic acid by acoustic or hydrodynamic cavitation in conjunction with the advanced Fenton process, Ultrason. Sonochem. 15 (2008) 416–419.

[29] Y.L. Song, J.T. Li, H. Chen, Degradation of CI Acid Red 88 aqueous solution by combination of Fenton's reagent & ultrasound irradiation, J. Chem. Technol. Biotechnol. 84 (2009) 578–583.

[30] C.G. Joseph, G.L. Puma, A. Bono, D. Krishnaiah, Sonophotocatalysis in advanced oxidation process: a short review, Ultrason. Sonochem. 16 (2009) 583–589.

[31] V.K. Saharan, A.B. Pandit, P.S.S. Kumar, S. Anandan, Hydrodynamic cavitation as an advanced oxidation technique for the degradation of Acid Red 88 dye, Ind. Eng. Chem. Res. 51 (2011) 1981–1989.

[32] G. Cravotto, P. Cintas, Harnessing mechanochemical effects with ultrasound-induced reactions, Chem. Sci. 3 (2012) 295–307.

[33] M. Quintana, M. Grzelczak, K. Spyrou, B. Kooi, S. Bals, G.V. Tendeloo, P. Rudolf, M. Prato, Production of large graphene sheets by exfoliation of graphite under high power ultrasound in the presence of tiopronin, Chem. Commun. 48 (2012) 12159–12161.

[34] K.P. Mishra, P.P. Gogate, Intensification of degradation of Rhodamine B using hydrodynamic cavitation in the presence of additives, Sep. Purif. Technol. 75 (2010) 385–391.

[35] P. Braeutigam, M. Franke, R.J. Schneider, A. Lehmann, A. Stolle, B. Ondruschka, Degradation of carbamazepine in environmentally relevant concentrations in water by hydrodynamic-acoustic-cavitation (HAC), Water Res. 46 (2012) 2469–2477.

[36] M.V. Bagal, P.R. Gogate, Degradation of 2,4-dinitrophenol using a combination of hydrodynamic cavitation, chemical and advanced oxidation processes, Ultrason. Sonochem. 20 (2013) 1226–1235.

[37] B. Yang, J.N. Zuo, X.H. Tang, F. Liu, X. Yu, X.Y. Tang, H. Jiang, L.L. Gan, Effective ultrasound electrochemical degradation of methylene blue wastewater using a nanocoated electrode, Ultrason. Sonochem. 21 (2014) 1310–1317.

[38] L. Zhao, J. Ma, X.D. Zhai, Enhanced mechanism of catalytic ozonation by ultrasound with orthogonal dual frequencies for the degradation of nitrobenzene in aqueous solution, Ultrason. Sonochem. 17 (2010) 84–91.

[39] L. Zhao, W.C. Ma, J. Ma, J.J. Yang, G. Wen, Z.Z. Sun, Characteristic mechanism of ceramic honeycomb catalytic ozonation enhanced by ultrasound with triple frequencies for the degradation of nitrobenzene in aqueous solution, Ultrason. Sonochem. 21 (2014) 104–112.

[40] A.G. Chakinala, P.R. Gogate, A.E. Burgess, D.H. Bremner, Industrial wastewater treatment using hydrodynamic cavitation and heterogeneous advanced Fenton processing, Chem. Eng. J. 152 (2009) 498–502.

[41] A.Q. Wang, W.L. Guo, F.F. Hao, X.X. Yue, Y.Q. Leng, Degradation of Acid Orange 7 in aqueous solution by zero-valent aluminum under ultrasonic irradiation, Ultrason. Sonochem. 21 (2014) 572–575.

[42] H.L. Lien, C.C. Yu, Y.C. Lee, Perchlorate removal by acidified zero-valent aluminum and aluminum hydroxide, Chemosphere 80 (2010) 888–893.

[43] H.H. Zhang, B.P. Cao, W.P. Liu, K.D. Lin, J. Feng, Oxidative removal of acetaminophen using zero valent aluminum-acid system: efficacy, influencing factors, and reaction mechanism, J. Environ. Sci. 24 (2012) 314–319.

[44] K.D. Lin, J.J. Cai, J.Q. Sun, X.L. Xue, Removal of 2,4-dichlorophenol by aluminium/O$_2$/acid system, J. Chem. Technol. Biotechnol. 15 (2013) 872–879.

[45] M. Arulkumar, P. Sathishkumar, T. Palvannan, Optimization of Orange G dye adsorption by activated carbon of *Thespesia populnea* pods using response surface methodology, J. Hazard. Mater. 186 (2010) 827–834.

[46] I.D. Mall, V.C. Srivastava, N.K. Agarwal, Removal of Orange-G and Methyl Violet dyes by adsorption onto bagasse fly ash kinetic study and equilibrium isotherm analyses, Dyes Pigments 69 (2005) 210–223.

[47] J. Madhavan, F. Grieser, M. Ashokkumar, Degradation of orange-G by advanced oxidation processes, Ultrason. Sonochem. 17 (2009) 338–343.

[48] L. Pereira, A.V. Coelho, C.A. Viegas, M.M. Correia dos Santos, M.P. Robalo, L.O. Martins, Enzymatic biotransformation of the azo dye Sudan Orange G with bacterial CotA-laccase, J. Biotechnol. 139 (2008) 68–77.

[49] H. Lachheb, E. Puzenat, A. Houas, M. Ksibi, E. Elaloui, C. Guillard, J.M. Herrmann, Photocatalytic degradation of various types of dyes (Alizarin S, Crocein Orange G, Methyl Red, Congo Red, Methylene Blue) in water by UV-irradiated titania, Appl. Catal. B 39 (2002) 75–90.

[50] J.H. Sun, L.P. Qiao, S.P. Sun, G.L. Wang, Photocatalytic degradation of Orange G on nitrogen-doped TiO$_2$ catalysts under visible light and sunlight irradiation, J. Hazard. Mater. 155 (2007) 312–319.

[51] J. Sun, X. Wang, J. Sun, R. Sun, S. Sun, L.P. Qiao, Photocatalytic degradation and kinetics of Orange G using nano-sized Sn(IV)/TiO$_2$/AC photocatalyst, J. Mol. Catal. A 260 (2006) 241–246.

[52] X.R. Xu, X.Z. Li, Degradation of azo dye Orange G in aqueous solutions by persulfate with ferrous ion, Sep. Purif. Technol. 72 (2010) 105–111.

[53] S.P. Sun, C.J. Li, J.H. Sun, S.H. Shi, M.H. Fan, Q. Zhou, Decolorization of an azo dye Orange G in aqueous solution by Fenton oxidation process: effect of system parameters and kinetic study, J. Hazard. Mater. 161 (2008) 1052–1057.

[54] H. Bader, V. Sturzenegger, J. Hoigné, Photometric method for the determination of low concentrations of hydrogen peroxide by the peroxidase catalyzed of N,N-diethyl-p-phenylenediamine (DPD), Water Res. 22 (1988) 1109–1115.

[55] L. Soler, J. Macanàs, M. Mu'noz, J. Casado, Aluminum and aluminum alloys as sources of hydrogen for fuel cell applications, J. Power Sources 169 (2007) 144–149.

[56] J.M. Campos-Martin, G. Blanco-Brieva, J.L.G. Fierro, Hydrogen peroxide synthesis: an outlook beyond the anthraquinone process, Angew. Chem. 45 (2006) 6962–6984.

[57] W.P. Liu, H.H. Zhang, B.P. Cao, K. Lin, J. Gan, Oxidative removal of bisphenol A using zero valent aluminum acid system, Water Res. 45 (2011) 1872–1878.

[58] H. Mei, B.W. Mei, T.F. Yen, A new method for obtaining ultra-low sulfur diesel fuel via ultrasound assisted oxidative desulfurization, Fuel 82 (2003) 405–414.

[59] N.H. Ince, G.T. Güyer, Impacts of pH and molecular structure on ultrasonic degradation of azo dyes, Ultrasonics 42 (2004) 591–596.

[60] J. Madhavan, F. Grieser, M. Ashokkumar, Degradation of orange-G by advanced oxidation processes, Ultrason. Sonochem. 17 (2010) 338–343.

[61] S. Vajnhandl, A.M.L. Marechal, Case study of the sonochemical decolouration of textile azo dye Reactive Black 5, J. Hazard. Mater. 12 (2007) 329–335.

[62] P.V. Nidheesh, R.J. Gandhimathi, S.T. Ramesh, Degradation of dyes from aqueous solution by Fenton processes: a review, Environ. Sci. Pollut. Res. (2013) 2099–2132.

[63] M.Q. Cai, M.C. Jin, L.K. Weavers, Analysis of sonolytic degradation products of azo dye Orange G using liquid chromatography–diode array detection–mass spectrometry, Ultrason. Sonochem. 18 (2011) 1068–1076.

[64] T. Leong, K. Yasui, K. Kato, D. Harvie, M. Ashokkumar, S. Kentish, Effect of surfactants on single bubble sonoluminescence behavior and bubble surface stability, Phys. Rev. E 89 (2014) 043–047.

[65] F. Ahmedchekkat, M.S. Medjram, M. Chiha, A. Mahmoud, A. Albsoul, Sonophotocatalytic degradation of Rhodamine B using a novel reactor geometry: effect of operating conditions, Chem. Eng. J. 178 (2011) 244–251.

[66] M. Siddique, R. Farooq, G.J. Price, Synergistic effects of combining ultrasound with the Fenton process in the degradation of Reactive Blue 19, Ultrason. Sonochem. 21 (2014) 572–575.

[67] P. Kanthale, M. Ashokkumar, F. Grieser, Sonoluminescence, sonochemistry (H$_2$O$_2$ yield) and bubble dynamics: frequency and power effects, Ultrason. Sonochem. 15 (2008) 143–150.

[68] A. Brotchie, F. Grieser, M. Ashokkumar, Effect of power and frequency on bubble-size distributions in acoustic cavitation, Phys. Rev. Lett. 102 (2009) 084–087.

[69] J.W. Kang, H.M. Hung, A. Lin, M.R. Hoffmann, Sonolytic destruction of methyl tert-Butyl ether by ultrasonic irradiation: the role of O$_3$, H$_2$O$_2$, frequency, and power density, Environ. Sci. Technol. 33 (1999) 3199–3205.

[70] M.O. Lamminen, H.W. Walker, L.K. Weavers, Mechanisms and factors influencing the ultrasonic cleaning of particle-fouled ceramic membranes, J. Membr. Sci. 237 (2004) 213–223.